The Hedgehog receptor Patched1 regulates myeloid and lymphoid progenitors by distinct cell-extrinsic mechanisms

Sarah L. Siggins,[1] Nhu-Y N. Nguyen,[1] Matthew P. McCormack,[1,2] Sumitha Vasudevan,[1] Rehan Villani,[3] Stephen M. Jane,[1,2] Brandon J. Wainwright,[3] and David J. Curtis[1,2]

[1]Rotary Bone Marrow Research Laboratories, Royal Melbourne Hospital, Parkville; [2]Department of Medicine, University of Melbourne, Parkville; and [3]Institute for Molecular Bioscience, The University of Queensland, Brisbane, Australia

Hedgehog (Hh) ligands bind to the Patched1 (Ptch1) receptor, relieving repression of Smoothened, which leads to activation of the Hh signaling pathway. Using conditional *Ptch1* knockout mice, the aim of this study was to determine the effects of activating the Hh signaling pathway in hematopoiesis. Surprisingly, hematopoietic-specific deletion of *Ptch1* did not lead to activation of the Hh signaling pathway and, consequently, had no phenotypic effect. In contrast, deletion of *Ptch1* in nonhematopoietic cells produced 2 distinct hematopoietic phenotypes. First, activation of Hh signaling in epithelial cells led to apoptosis of lymphoid progenitors associated with markedly elevated levels of circulating thymic stromal lymphopoietin. Second, activation of Hh signaling in the bone marrow cell niche led to increased numbers of lineage-negative c-kit$^+$ Sca-1$^+$ bone marrow cells and mobilization of myeloid progenitors associated with a marked loss of osteoblasts. Thus, deletion of *Ptch1* leads to hematopoietic effects by distinct cell-extrinsic mechanisms rather than by direct activation of the Hh signaling pathway in hematopoietic cells. These findings have important implications for therapeutics designed to activate the Hh signaling pathway in hematopoietic cells including hematopoietic stem cells. (Blood. 2009;114:995-1004)

Introduction

In vertebrates, the Hedgehog (Hh) signaling pathway is regulated by 3 Hh ligands: Sonic hedgehog (Shh), Indian hedgehog (Ihh), and Desert hedgehog. In the absence of Hh ligands, the transmembrane receptor Patched1 (Ptch1) inhibits the activity of a second receptor known as Smoothened (Smo). Binding of Hh ligands to Ptch1 relieves the repression on Smo, thus allowing pathway activation to proceed by nuclear translocation of activator and repressor forms of the target-gene Gli family of zinc finger transcription factors.[1]

The Hh pathway is important for the development of numerous cell lineages, including hematopoiesis. In zebrafish, Hh signaling is required for the development of definitive hematopoiesis while in *Drosophila*, Hh signaling maintains hematopoietic stem cell (HSC) quiescence.[2,3] However, effective hematopoietic reconstitution by $Smo^{-/-}$ fetal liver cells suggests that Hh signaling is not required for maintenance of adult HSCs.[4] In addition to a role in HSCs, studies of *Shh*-null and conditional *Smo*-null mice suggest Hh signaling is required for normal T-cell development.[5,6]

The effects of increased Hh signaling on hematopoiesis are not well defined. Increased Hh signaling by loss of function mutations of Ptch1 lead to increased proliferation of stem or progenitor cells of the skin and brain, ultimately leading to basal cell carcinomas and medulloblastomas, respectively.[7,8] A similar expansion of HSCs or progenitors might also occur by activating the Hh pathway, raising both therapeutic and cancer stem cell implications.[9] However, experimental models designed to address the effects of increased Hh signaling in hematopoiesis have been hampered by poor in vitro and in vivo bioavailability of Hh ligands. Incubation of primitive hematopoietic progenitors with Hh ligands, either alone or on stromal feeders, increases the numbers of nonobese diabetic–severe combined immunodeficiency (NOD/SCID) repopulating cells, although this could be an indirect effect.[10,11] An alternate method of studying the effects of activating the Hh pathway is through genetic deletion of *Ptch1*. Whereas *Ptch1*-null embryos die before the development of definitive hematopoiesis,[12] germline *Ptch1*-heterozygous mice have increased numbers of HSC-enriched, lineage-negative c-kit$^+$Sca-1$^+$ (LKS) bone marrow (BM) cells due to increased cell cycling.[13] Noncompetitive transplant assays of *Ptch1*-heterozgous BM cells into NOD/SCID mice suggested that this aberrant cell cycling improved early (5 weeks) repopulating capacity at the expense of longer-term (8 weeks) repopulating capacity.[13] Uhmann et al reported a conditional deletion of *Ptch1* in adult hematopoiesis using a ubiquitous Cre under the control of tamoxifen.[14] Homozygous deletion of *Ptch1* led to increased numbers of LKS, but functional assays were not performed. In this model, deletion of *Ptch1* also led to loss of B and T cells, although transplant assays into $Rag2^{-/-}$ $\gamma^{-/-}$ mice suggested that these lymphoid defects were cell extrinsic.[14]

Using inducible and tissue-specific deletion of *Ptch1* on a congenic C57BL/6J background, the aim of this study was to determine the cell-intrinsic and cell-extrinsic hematopoietic effects of activation of the Hh signaling pathway. Surprisingly, we found that deletion of *Ptch1* in hematopoietic cells did not activate the Hh signaling pathway, and consequently had no phenotypic effects. In contrast, activation of the Hh signaling pathway by deletion of *Ptch1* in epithelial cells led to apoptosis of lymphoid progenitors,

Submitted March 2, 2009; accepted May 17, 2009. Prepublished online as *Blood* First Edition paper, May 29, 2009; DOI 10.1182/blood-2009-03-208330.

The online version of this article contains a data supplement.

The publication costs of this article were defrayed in part by page charge payment. Therefore, and solely to indicate this fact, this article is hereby marked "advertisement" in accordance with 18 USC section 1734.

whereas deletion of *Ptch1* in the BM cell niche led to increased numbers of LKS and circulating myeloid progenitors. High levels of circulating thymic stromal lymphopoietin (TSLP) and loss of osteoblasts may explain these lymphoid and myeloid progenitor cell defects, respectively. These findings have important implications for therapeutics designed to activate the Hh signaling pathway in hematopoietic cells, including HSCs.

Methods

Generation of Ptch1-null mice

Ptch1^{fl} mice[15] were backcrossed onto a C57BL/6J background for 10 generations. Congenic *Ptch1*^{fl} mice were bred with transgenic mice expressing Cre recombinase under the control of the interferon-inducible promoter, *Mx1*.[16] *Ptch1*$^{fl/fl}$, *MxPtch1*$^{+/fl}$, and *MxPtch1*$^{fl/fl}$ mice were injected with 300 μg polyinosinic-polycytidylic acid (poly(I:C); Sigma-Aldrich) dissolved in normal saline intraperitoneally on alternate days for 3 doses. Deletion of *Ptch1* in HSCs was achieved by breeding *Ptch1*^{fl} mice with transgenic mice expressing the tamoxifen-inducible Cre-ER recombinase under the control of the stem cell leukemia (*Scl*) stem cell enhancer (HSC-Scl-CreER).[17] For inducing Cre-ER recombinase, *SclPtch1* mice were treated with 3 intraperitoneal injections of 10 mg tamoxifen (Sigma-Aldrich) diluted in corn oil (50 mg/mL). *CD19Cre* mice[18] and *LckCre* mice[19] were backcrossed onto the C57BL/6 background. Deletion of *Ptch1* in epithelial cells was achieved by crossing *Ptch1*^{fl} mice with Keratin 14 (K14) Cre transgenics.[20] Female CD45.1 (B6.SJL(Ptprca[Ly5.1])) mice were purchased from the Walter and Eliza Hall Institute for Medical Research (WEHI) Animal House Facility. Melbourne Health and the University of Melbourne animal ethics committees approved all animal experiments. Deletion of the *Ptch1*^{fl} allele was confirmed by either Southern blot or polymerase chain reaction (PCR). For Southern blot analysis, genomic DNA was digested by either *Xba*I or *Bam*HI and then probed with a *Sac*I/*Nsi*I fragment from a 3-kb *Spe*I fragment of the second intron of *Ptch1*.[15] Primers used for PCR genotyping are shown in supplemental Table 1, available on the *Blood* website (see the Supplemental Materials link at the top of the online article).

Sample preparation, histology, and immunohistochemistry

All analyses were performed at least 4 weeks after poly(I:C) administration to avoid the effects of the interferon response. For whole blood counts, 250 μL of blood was collected from the retro-orbital plexus into tubes containing potassium EDTA (Sarstedt), and blood counts analyzed using an Advia 2120 automated hematologic analyzer (Bayer). BM cells were harvested by flushing femurs with mouse tonicity (MT)–PBS/2% fetal bovine serum (FBS). Thymi and spleens were filtered through 45-μm nylon screens to generate single-cell suspensions. Histologic analyses were done on paraffin-embedded skin fixed with 10% neutral buffered formalin. All sections were stained with hematoxylin and eosin (H&E). Immunohistochemistry for Keratin 14 (anti–Keratin 14 [AF64]; PRB-155P; Covance Research Products) was performed using standard immunohistochemistry (IHC) techniques. Images were acquired using a Nikon Eclipse 80i microscope equipped with a 40×/0.75 NA objective lens. Images were captured with a Nikon DXM1200C digital camera, and figures were created without manipulation in Adobe Photoshop 10.0.1 (Adobe Systems).

Flow cytometric analysis and sorting

Antibodies used for analyses were obtained from BD Pharmingen: CD8a (clone 53-6.7), CD45.2 (104), annexin V, B220 (RA3-6B2), IgM (AF6-78), and Sca-1 (E13-161-7) as fluoroscein isothiocyanate (FITC) conjugates; CD4 (GK1.5), Mac-1a (M1/70), CD19 (1D3), CD21 (7G6), CD45.1 (A20), and c-kit (2B8) as phycoerythrin (PE) conjugates; B220 and c-kit as allophycocyanin (APC) conjugates; and biotinylated CD3e (145-2C11), CD4, CD8, CD23 (B3B4), CD11b, B220, Gr-1 (RB6-8C5), and TER-119. Second-stage fluorescent reagents were either SAv-APC or SAv-PerCP-Cy5.5. The appropriate conjugated rat anti–mouse isotypes were used as negative controls. Viability was determined by exclusion of propidium iodide (Sigma-Aldrich). For cell-cycle analysis, sorted cells were fixed in 70% ethanol, washed with PBS, and stained with ice-cold 2 mg/mL Hoechst 33342 (Molecular Probes) and 4 mg/mL Pyronin Y (Polysciences) for 20 minutes before analysis with a BD LSR Benchtop flow cytometer (BD Biosciences). For isolation of LKS and lineage-negative c-Kit^{+}Sca-1^{-} (LK) cell fractions, cell sorting of immature BM cells after immunomagnetic bead depletion of lineage marker–positive BM cells was performed before sorting on a FACSVantage SE system (BD Biosciences). The purity of sorted cells was determined by reanalyzing a small sample of the collected cells and was 80% to 90%. All data were analyzed using a WEHI in-house program, Weasel version 2.3.

Transplant assays

Competitive repopulation assays were performed as previously described.[21] Female CD45.1 mice were used as recipients and as a source of competitor BM cells (2×10^6). Donor BM cells (2×10^6) were obtained from *MxPtch1*$^{\Delta/\Delta}$, *MxPtch1*$^{\Delta/+}$, or *Ptch1*$^{fl/fl}$ mice 6 to 8 weeks after poly(I:C). Each transplant inoculum was injected into a minimum of 3 recipients. Secondary recipients received 10^7 BM cells from primary recipients.

Real-time PCR

RNA from sorted cells was isolated using TRIZol (Invitrogen), and genomic DNA was removed using Turbo DNA-free kit (Ambion). Reverse transcription of 2 μg DNA-free RNA into cDNA was carried out with the Omniscript Reverse Transcription Kit (QIAGEN). Real-time quantitative (Q)–PCR 20-μL reactions each contained 1 μL cDNA, the fluorescent DNA binding dye SYBR green (Molecular Probes), and specific primers (supplemental Table 1) were used for all hematopoietic tissues. Amplification was performed in a RotorGene 2000 PCR instrument (Corbett Research) at 95°C for 5 minutes followed by 40 cycles of 15 seconds at 94°C, 30 seconds at 60°C, and 30 seconds at 72°C, and 30 seconds at 82°C. SYBR Green dye intensity was analyzed using the RotorGene 200 software, and all Ct values were normalized to HPRT. For expression of TSLP and Gli1 in skin and whole-bone samples, Taqman MGB probes and FAM dye-labeled Expression Systems were used (Applied Biosystems). Preincubation was performed in a Roche LightCycler 480 II (Roche) at 50°C for 2 minutes followed by 20 seconds at 95°C. Amplification was performed at 95°C for 3 seconds followed by 30 seconds at 60°C for 45 cycles before cooling at 40°C for 30 seconds.

Progenitor assays

BM, spleen, and peripheral blood cells were cultured in 0.3% agar cultures and analyzed as previously described.[22] Recombinant cytokines were used at the following concentrations: 10 ng/mL mIL-3, 50 ng/mL mIL-6, and 50 ng/mL rSCF (R&D Systems).

Cell culture

Mouse mesodermal cells derived from 14- to 17-day-old embryos, C3H/10T1/2 (C3H), were obtained from ATCC. Cells were grown in Dulbecco modified Eagle medium (DMEM) supplemented with 10% (vol/vol) FBS and 100 U/mL penicillin/streptomycin and were cultured in 5% CO_2 and 95% air. For experiments, cells were seeded into 12-well plates at 70 000 cells/well and allowed to attach overnight. The next day, Shh-conditioned medium was added at a 1:5 dilution with 5% FCS DMEM and incubated on the cells for 3 days. Cells were then harvested for RNA using TRIZol.

TSLP immunoassay

Serum samples were collected from kill bleeds of mice. Serum TSLP levels were measured using the Quantikine mouse TSLP immunoassay (catalog no. MTLP00; R&D Systems).

Results

Deletion of Ptch1 in adult mice leads to death of B- and T-cell progenitors

To delete *Ptch1* in adult hematopoiesis, we intercrossed *MxCre* transgenic mice with animals carrying a conditional "floxed" (fl) allele of *Ptch1* (*Ptch1*^{fl}).[15] Deletion of the *Ptch1*^{fl} allele (*Ptch1*$^{\Delta}$) early in development is embryonic lethal and phenocopies the germline *Ptch1*-null mice.[12,15] *Ptch1*-null (*MxPtch1*$^{\Delta/\Delta}$) hematopoiesis was generated by treating *MxPtch1*$^{fl/fl}$ mice with poly(I:C). Control animals, also treated with poly(I:C), included *Ptch1*-wild-type mice (*Ptch1*$^{fl/fl}$) and *Ptch1*-heterozygous mice (*MxPtch1*$^{+/\Delta}$). Deletion of one *Ptch1* allele had no effect on hematopoiesis and therefore, in some experiments, *MxPtch1*$^{+/\Delta}$ mice were used as controls. Southern blot analysis of hematopoietic organs confirmed more than 90% deletion of the targeted *Ptch1*^{fl} allele (Figure 1A).

Hematopoiesis of *MxPtch1*$^{\Delta/\Delta}$ mice was examined 4 to 6 weeks after poly(I:C), a time-point after resolution of the interferon effects from poly(I:C). Analysis of peripheral blood counts of *MxPtch1*$^{\Delta/\Delta}$ mice revealed a significant increase in neutrophils but no effect on hemoglobin, lymphocyte count, or platelet count (Table 1). The cell surface markers on B220^{+} B cells of the BM and spleen used to enumerate B-cell subsets are shown in supplemental Figure 1A. Although numbers of pro-B cells (B220^{lo}CD19^{-}) were normal, *MxPtch1*$^{\Delta/\Delta}$ mice had a 4-fold loss of pre-BI cells (B220^{lo}c-kit^{+}) and pre-BII cells (B220^{lo}CD25^{+}) in the BM (Figure 1B-C). Despite loss of pre-B cells, deletion of *Ptch1* did not significantly affect the numbers of immature (B220^{lo}IgM^{+}) and recirculating (B220^{hi}IgD^{+}) B cells within the BM. B-cell subset analysis of the spleen revealed a 3-fold reduction in the proportion of follicular B cells (supplemental Figure 1B). However, absolute numbers of follicular B cells were normal because the spleen size of *MxPtch1*$^{\Delta/\Delta}$ mice was increased 3-fold due to increased numbers of myeloid cells (supplemental Figure 1C). The loss of BM pre-B cells was due to increased cell death, as this population, but not recirculating B cells, displayed increased expression of annexin V (Figure 1D). In contrast, Ptch1 was not required for cell-cycle control or maturation of pre-B cells, as determined by Hoechst staining (supplemental Figure 1D) and in vivo BrdU labeling (supplemental Figure 1E), respectively. Thus, deletion of *Ptch1* by the MxCre transgene leads to death of BM pre-B cells.

In addition to B-cell defects, *MxPtch1*$^{\Delta/\Delta}$ mice developed thymic atrophy (Figure 2A). Flow cytometry of thymic T-cell subsets demonstrated significant loss of the CD4^{+}CD8^{+} double-positive (DP) cells (Figure 2B). Although the proportions of the other subsets (double negative [DN] and single positive) were relatively increased, the absolute number of all T-cell subsets was significantly reduced in the *MxPtch1*$^{\Delta/\Delta}$ thymi (Figure 2C). The proportions of DN subsets were unaffected by deletion of Ptch1 (supplemental Figure 2). Similar to the B-cell phenotype, increased expression of annexinV^{+} on DP cells indicated increased apoptosis (Figure 2D). Thus, deletion of *Ptch1* by the *MxCre* transgene leads to death of thymocytes, especially DP cells.

Deletion of Ptch1 promotes cell cycle and mobilization of immature myeloid progenitors

To examine the effects of *Ptch1* deletion on myelopoiesis, we measured myeloid progenitors within the BM, spleen, and peripheral blood of *MxPtch1*$^{\Delta/\Delta}$ mice. There was no change in either the numbers or types of myeloid progenitors within the BM (Table 2).

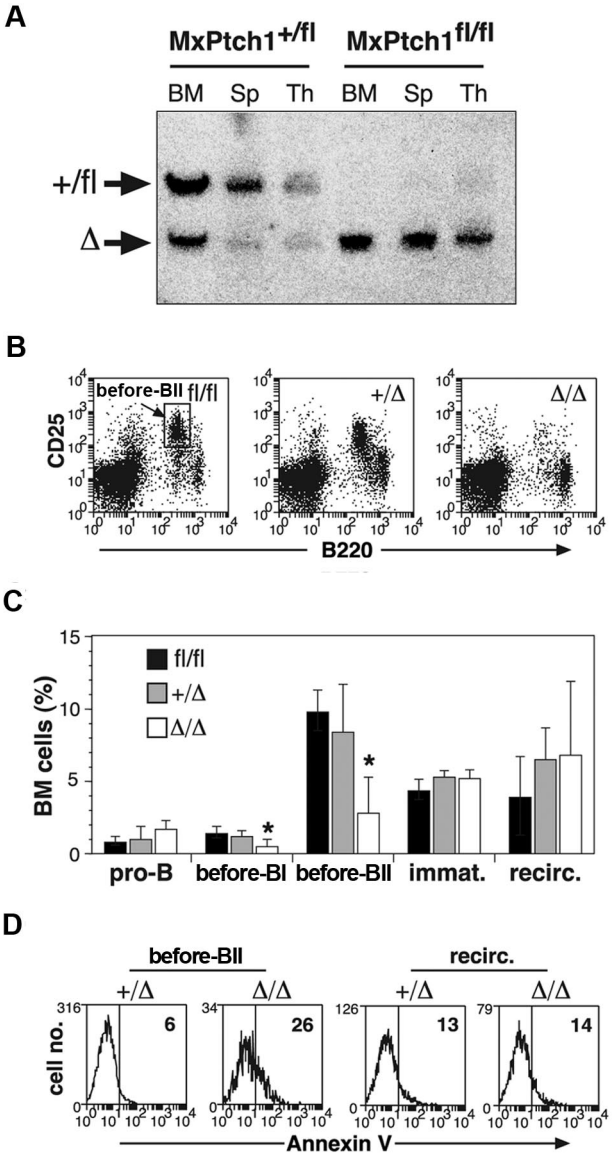

Figure 1. B-cell defects in the absence of *Ptch1*. (A) Southern blot analysis for *Ptch1* deletion status. Bone marrow (BM), spleen (Sp), and thymus (Thy) from *MxPtch1*$^{+/fl}$ and *MxPtch1*$^{fl/fl}$ mice harvested 4 weeks after administration of poly(I:C). Wild-type *Ptch1* allele (+) and loxP-flanked *Ptch1* allele (fl) have the same size band. Deleted *Ptch1*^{fl} allele (Δ). (B) Dot plots of BM cells stained with B220 and CD25. The *MxPtch1*$^{\Delta/\Delta}$ dot-plot is an example of a severely affected animal. (C) B-cell subsets in BM from *Ptch1*-wild-type (*Ptch1*$^{fl/fl}$), heterozygous (*MxPtch1*$^{+/\Delta}$) and null (*MxPtch1*$^{\Delta/\Delta}$) mice: see supplemental Figure 1 for definitions of B-cell subsets. Mean plus SD calculated from 5 mice of each genotype. $^{*}P < .05$ by one-way ANOVA. (D) Annexin V expression on pre-BII and recirculating B cells within the BM. The mean percentage of annexin V^{+} cells calculated from 3 mice for each genotype is shown.

However, the spleen and peripheral blood of *MxPtch1*$^{\Delta/\Delta}$ mice contained at least 10-fold more granulocyte-macrophage progenitors (Figure 3A). To assess the consequences of *Ptch1* deletion on HSCs, we enumerated early progenitor populations by flow cytometry. *MxPtch1*$^{\Delta/\Delta}$ mice had a 3-fold increase in numbers of LKS cells, a fraction enriched for HSCs and multipotent myeloid progenitors (Figure 3B-C). However, the numbers of LK cells, a cell fraction containing more mature myeloid-restricted progenitors, was not significantly increased by deletion of *Ptch1*, consistent with normal numbers of BM myeloid progenitors formed in 7-day culture assays.

As deletion of *Ptch1* promotes cycling of cerebellar neuronal precursors,[23] we examined the cell-cycle status of sorted LKS

Table 1. Peripheral blood counts in *MxPtch1* mice

Genotype	Hb, g/L	WCC, 10^9/L	Platelets, 10^9/L	Neutrophils, 10^9/L	Lymphocytes, 10^9/L
fl/fl (n = 4)	151 ± 7	9.6 ± 1.9	1101 ± 281	1.0 ± 0.6	7.7 ± 2.2
+/Δ (n = 7)	155 ± 15	7.7 ± 2.8	1169 ± 219	0.6 ± 0.3	6.5 ± 2.5
Δ/Δ (n = 7)	148 ± 29	10.7 ± 4.7	1510 ± 377	3.8 ± 3.8*	6.4 ± 1.8

Peripheral blood counts of *Ptch1*$^{fl/fl}$, *MxPtch1*$^{+/\Delta}$, and *MxPtch1*$^{\Delta/\Delta}$ *mice 4 to 6 weeks after poly(I:C). Hb indicates hemoglobin; and WCC, white cell count.*
*$P = .04$ by one-way ANOVA.

and LK subsets by staining with Hoechst and Pyronin dyes (Figure 3D). This analysis revealed a 2-fold increase in the number of cycling *MxPtch1*$^{\Delta/\Delta}$ LKS cells compared with *MxPtch1*$^{+/\Delta}$ LKS, and a corresponding reduction in quiescent (G_0) cells. In contrast, deletion of *Ptch1* had no effect on the cell-cycle status of the more mature LK cell fraction. The increased cycling of *MxPtch1*$^{\Delta/\Delta}$ LKS cells was associated with a 4-fold increase in expression of the major D-type cyclin expressed in LKS, cyclin D1 (Figure 3E). Overall, these results show that homozygous deletion of *Ptch1* by the *MxCre* transgene led to increased numbers of proliferating LKS cells and mobilization of myeloid progenitors.

Deletion of Ptch1 does not affect HSC activity

To address the functional consequences of deleting *Ptch1* on HSC activity, we performed competitive repopulation transplantation experiments. Donor mice (*MxPtch1*$^{fl/fl}$, *MxPtch1*$^{fl/+}$, *Ptch1*$^{fl/fl}$) were treated with poly(I:C) 6 weeks before transplantation. Competitor and recipient BM cells were distinguished from donor cells by the CD45.1 congenic marker. Despite increased numbers of LKS, homozygous deletion of *Ptch1* in the adult had no effect on short-term (4 weeks) repopulating activity of peripheral blood leukocytes (Figure 4A). Furthermore, analysis of BM repopulation 16 weeks after transplantation did not reveal any change in long-term HSC activity (Figure 4B). Secondary transplantation of donor *MxPtch1*$^{\Delta/\Delta}$ HSCs was also normal, indicating that Ptch1 does not regulate self-renewal of HSCs (Figure 4C). Thus, deletion of *Ptch1* in HSCs had no significant effect on HSC activity despite the altered cycling status of LKS cells.

Hematopoietic-specific deletion of Ptch1 demonstrates redundancy

Although the *MxCre* transgene efficiently deletes "floxed" genes in HSCs, it can also be induced in a wide range of nonhematopoietic cell types, including the liver, brain, and endothelial cells.[16,24] To examine the effects of deleting *Ptch1* specifically in hematopoietic cells, we used transgenic mice carrying the tamoxifen-inducible Cre-ER recombinase under the control of the SCL stem cell enhancer [HSC-SCL-Cre-ER(T)].[17] Genomic Southern blot analysis demonstrated more than 90% deletion of the *Ptch1*^{fl} allele in BM cells (Figure 5A). Despite this, *SclPtch1*$^{\Delta/\Delta}$ mice displayed normal numbers of LKS cells (Figure 5B), suggesting that the increased LKS cells seen in *MxPtch1* mice was not cell intrinsic. To achieve B cell–specific deletion of *Ptch1*, we used *CD19Cre* transgenic mice, which constitutively express Cre from the pre-B cell stage.[18] PCR genotyping confirmed more than 80% deletion of *Ptch1* in BM pre-BII cells (Figure 5C). Consistent with a cell-extrinsic B-cell defect in *MxPtch1*$^{\Delta/\Delta}$ mice, *CD19Ptch1*$^{\Delta/\Delta}$ mice had normal numbers of pre-B cells at 6 months of age (Figure 5D). To examine the effects of deleting *Ptch1* specifically in

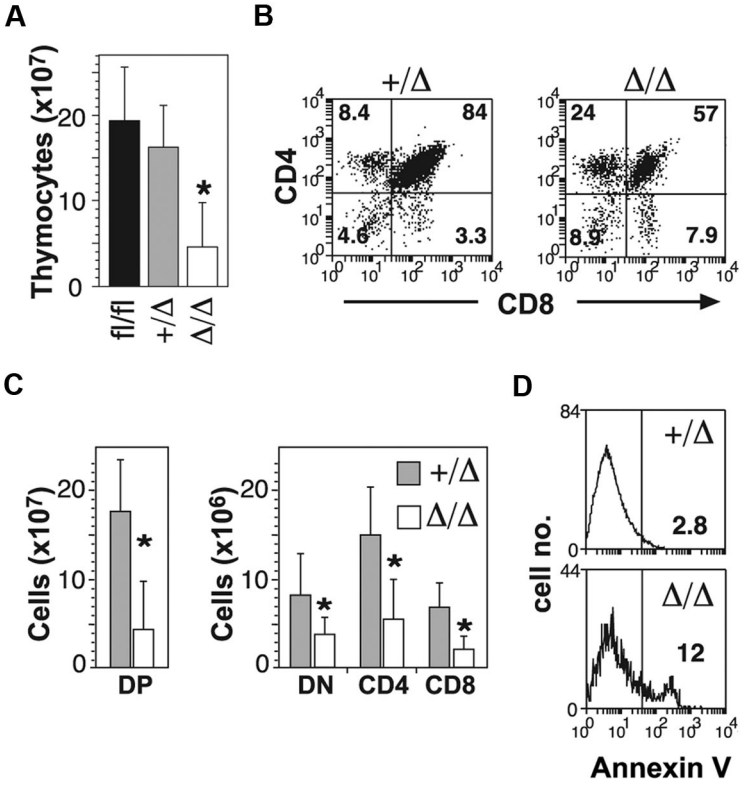

Figure 2. T-cell defects in the absence of *Ptch1*. (A) Total numbers of thymocytes (mean plus SD calculated from 8 mice of each genotype). *$P < .05$ by one-way ANOVA. (B) Representative dot-plots of T-cell subsets. The mean percentage shown for each subset was calculated from 8 mice of each genotype. (C) Total numbers of T-cell subsets: $CD4^-CD8^-$ double negative (DN); $CD4^+CD8^+$ double positive (DP); $CD4^+$ single positive (CD4); $CD8^+$ single positive (CD8). Mean plus SD calculated from 8 mice of each genotype. *$P < .05$ by 2-tailed Mann-Whitney test. (D) Annexin V expression on DP thymocytes. The mean percentage of annexin V^+ calculated from 3 mice for each genotype is shown.

Table 2. Types of bone marrow progenitors in *MxPtch1*$^{\Delta/\Delta}$ mice

Genotype	Colonies						
	Total	Granulocyte	GM	Macrophage	Megakaryocyte	GEMM	Blast
+/Δ (n = 3)	62 ± 12	13 ± 6	23 ± 8	12 ± 2	7 ± 3	3 ± 2	4 ± 2
Δ/Δ (n = 3)	87 ± 18	14 ± 2	26 ± 4	21 ± 7	12 ± 5	8 ± 4	6 ± 2

Mean and SD from 3 mice plated in triplicate.
GM indicates granulocyte/macrophage mixed; and GEMM, granulocyte/erythroid/macrophage/megakaryocyte mixed.

T cells, we used the *LckCre* transgenic mice.[19] Despite highly efficient deletion of *Ptch1* in the thymus of *LckPtch1*$^{\Delta/\Delta}$ mice, these animals exhibited normal thymic cellularity (Figure 5E) and no change in the proportion of T-cell subsets at 6 months of age (Figure 5F).

Despite efficient deletion of *Ptch1* by hematopoietic-specific Cre transgenics, no hematopoietic effects were observed, suggesting that either activation of Hh signaling in hematopoiesis had no consequence or that, alternatively, deletion of *Ptch1* did not lead to inappropriate activation of Hh signaling in hematopoietic cells. To address these 2 alternatives, we examined the expression of Gli1 in our target cell populations by quantitative RT-PCR. As a positive control for activation of the Hh pathway, we used the mesenchymal cell line C3H treated with Shh-conditioned media, which produced a 50-fold increase in Gli1 mRNA (Figure 5G). Surprisingly, no significant increase in Gli1 expression was detected in freshly isolated pre-B cells from *CD19Ptch1*$^{\Delta/\Delta}$ mice or DP thymocytes from *LckPtch1*$^{\Delta/\Delta}$ mice (supplemental Figure 3). More importantly, Gli1 expression was not increased in sorted B-cell progenitors, thymocyte subsets, LKS cells, or LK cells from phenotypic *MxPtch1*$^{\Delta/\Delta}$ mice (Figure 5H). Thus, deletion of *Ptch1* did not lead to activation of the Hh signaling pathway in hematopoietic cells. Furthermore, the hematopoietic phenotype in *MxPtch1*$^{\Delta/\Delta}$ mice could not be attributed to cell-intrinsic activation of the Hh pathway.

Hematopoietic abnormalities are due to *Ptch1* deletion in nonhematopoietic cells

The absence of a phenotype in hematopoietic-specific Cre transgenics suggested that the phenotype in *MxPtch1*$^{\Delta/\Delta}$ mice was a cell-extrinsic defect due to activation of the Hh signaling pathway in nonhematopoietic cells. To address this possibility, we generated BM chimeras: lethally irradiated *MxPtch1*$^{fl/fl}$ mice were reconstituted with wild-type BM cells, and lethally irradiated wild-type mice were reconstituted with *MxPtch1*$^{fl/fl}$ BM cells (Figure 6A). At 4 to 8 weeks after transplantation, reconstituted mice were treated with poly(I:C) to delete *Ptch1*, either in nonhematopoietic cells including the cell niche (*MxPtch1*$^{fl/fl}$ recipient mice), or hematopoietic cells (*MxPtch1*$^{fl/fl}$ donor BM). Consistent with a cell-extrinsic mechanism, *MxPtch1*$^{\Delta/\Delta}$ mice reconstituted with wild-type BM displayed 3-fold more LKS, reduced pre-B cell numbers and marked loss of thymic cellularity compared with wild-type mice reconstituted with *MxPtch1*$^{\Delta/\Delta}$ BM (Figure 6B). Thus, deletion of *Ptch1* in nonhematopoietic cells explains both the lymphoid and myeloid abnormalities of *MxPtch1*$^{\Delta/\Delta}$ mice.

The BM cell niche contains cell types important for regulation of both HSCs and B-cell progenitors, including osteoblasts lining the endosteum.[25,26] We examined the bones of *MxPtch1*$^{\Delta/\Delta}$ mice for abnormalities that might explain the hematopoietic phenotype. Histologic examination of long bones from *MxPtch1*$^{\Delta/\Delta}$ mice revealed extensive thinning of cortical bone (Figure 6C), which

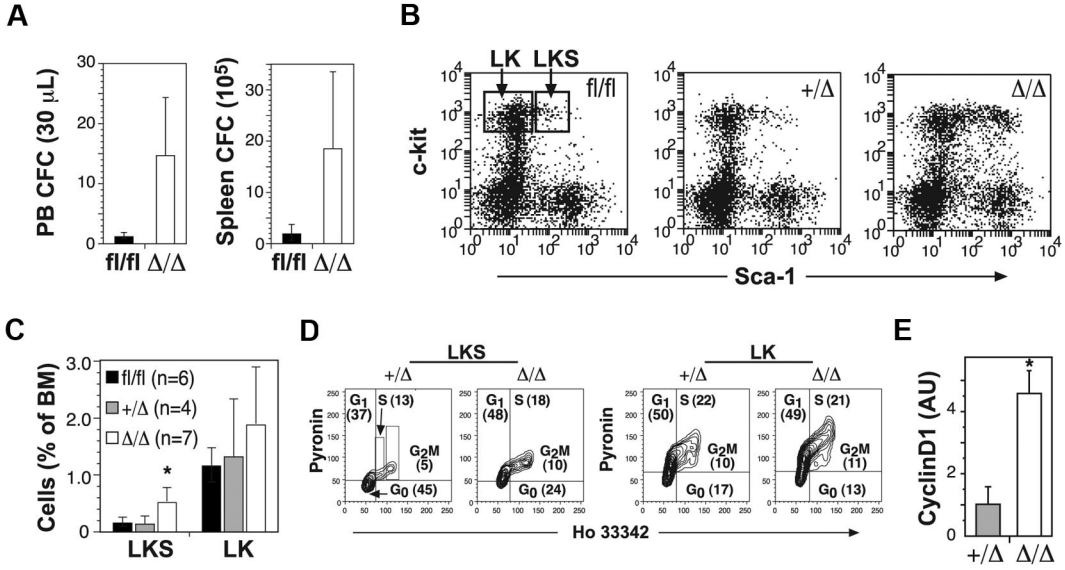

Figure 3. Increased cell cycle and mobilization of multipotent progenitors in the absence of *Ptch1*. (A) Numbers of circulating peripheral blood and spleen myeloid colony-forming cells in *Ptch1* wild-type (*Ptch1*$^{fl/fl}$) and null (*MxPtch1*$^{\Delta/\Delta}$) mice 4 to 6 weeks after poly(I:C). Mean plus SD calculated from 3 mice of each genotype. (B) Representative dot-plots for c-kit and Sca-1 expression on lineage-negative BM cells. Gates used to calculate proportions of LKS and LK cells are shown. (C) Proportions of LKS and LK cells expressed as a percentage of nucleated BM cells. The numbers of mice used to calculate the mean plus SD are shown in parentheses. *$P < .05$ by one-way ANOVA. (D) Cell-cycle analysis of FACS-isolated LKS and LK cells stained with Hoechst 33342 and Pyronin Y. The mean percentage of each stage of cell cycle calculated from 4 mice is shown. (E) Quantitative RT-PCR for cyclin D1 mRNA expression in LKS. The control samples have been normalized to 1, and the mean plus SD from 3 mice of each genotype are shown. *$P < .05$ by 2-tailed Mann-Whitney test.

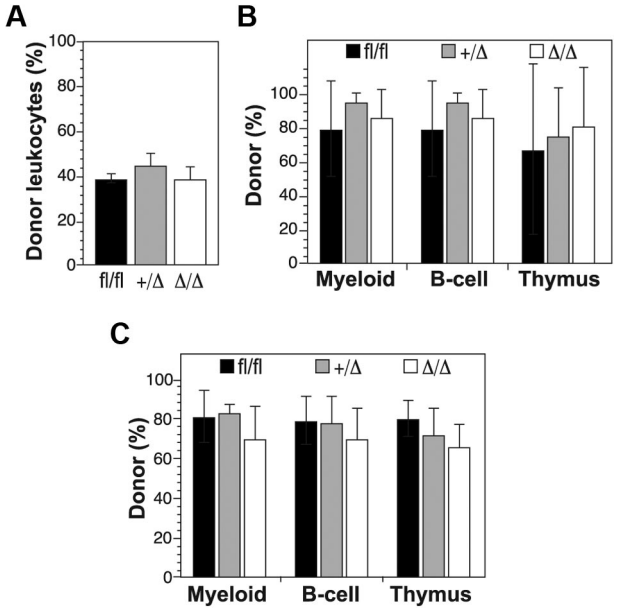

Figure 4. Competitive repopulation assays of *Ptch1*-null hematopoietic stem cells. (A) Donor leukocyte contribution in peripheral blood of recipient mice 4 weeks after transplantation with a 1:1 ratio of donor (*Ptch*$^{fl/fl}$, *MxPtch1*$^{+/\Delta}$, or *MxPtch1*$^{\Delta/\Delta}$) and wild-type CD45.1 competitor BM cells. Mean plus SD calculated from 4 recipients of each donor genotype. (B) Donor contribution 16 weeks after transplantation. Mice were killed to determine donor contribution to the myeloid lineage (Mac-1$^+$ BM cells), B-cell lineage (B220$^+$ BM cells), and T-cell lineage (CD4$^+$CD8$^+$ DP thymocytes). Mean plus SD calculated from 4 recipients of each donor genotype. (C) Donor contribution to hematopoiesis of secondary recipients that received transplants of BM cells from primary recipients shown in panel B. Mice were analyzed 12 weeks after transplantation. Mean plus SD calculated from 4 recipients of each donor genotype.

was confirmed by peripheral quantitative computer-aided tomography (supplemental Figure 4). Loss of cortical bone was associated with marked changes in osteoblasts: *MxPtch1*$^{\Delta/\Delta}$ bones had 4-fold fewer osteoblasts (Figure 6D), which were flat and elongated rather than the normal cuboidal shape (Figure 6E). In addition to impaired bone formation, *MxPtch1*$^{\Delta/\Delta}$ BM cells had increased expression of *RANKL* (Figure 6F), a cytokine that promotes bone resorption and mobilization of BM progenitors.[27]

MxCre is expressed in cells of the BM niche, although the specific cell types are poorly defined.[28,29] To determine whether *Ptch1* is deleted in osteoblasts, we isolated CD45$^-$Lin$^-$CD31$^-$CD51$^+$ osteoblasts by fluorescence-activated cell sorter (FACS) from *MxPtch1*-heterozygous (*MxPtch1*$^{+/\Delta}$) mice, which had normal numbers of osteoblasts. PCR genotyping demonstrated that the *MxCre* transgene deleted the *Ptch1*^{fl} allele in osteoblasts (Figure 6G).

Initial attempts to isolate osteoblasts from *MxPtch1*$^{\Delta/\Delta}$ mice yielded insufficient RNA for Gli1 expression. However, RNA prepared from whole bones revealed 3-fold more Gli1 in *MxPtch1*$^{\Delta/\Delta}$ bones (Figure 6H). Thus, deletion of *Ptch1* by *MxCre* leads to activation of the Hh signaling pathway in the BM cell niche.

Lymphoid defects are caused by activation of the Hh signaling pathway in epithelial cells

Ptch1 was deleted not only in osteoblasts but also in the basal cells of the skin. 6 to 8 weeks after poly(I:C), *MxPtch1*$^{\Delta/\Delta}$ mice developed ruffled coats that progressed to typical basal cell carcinoma of the skin (Figure 7A). These skin changes were due to marked activation of the Hh pathway: Gli1 mRNA levels were 10-fold more than that seen in Shh-treated C3H cells (Figure 7B).

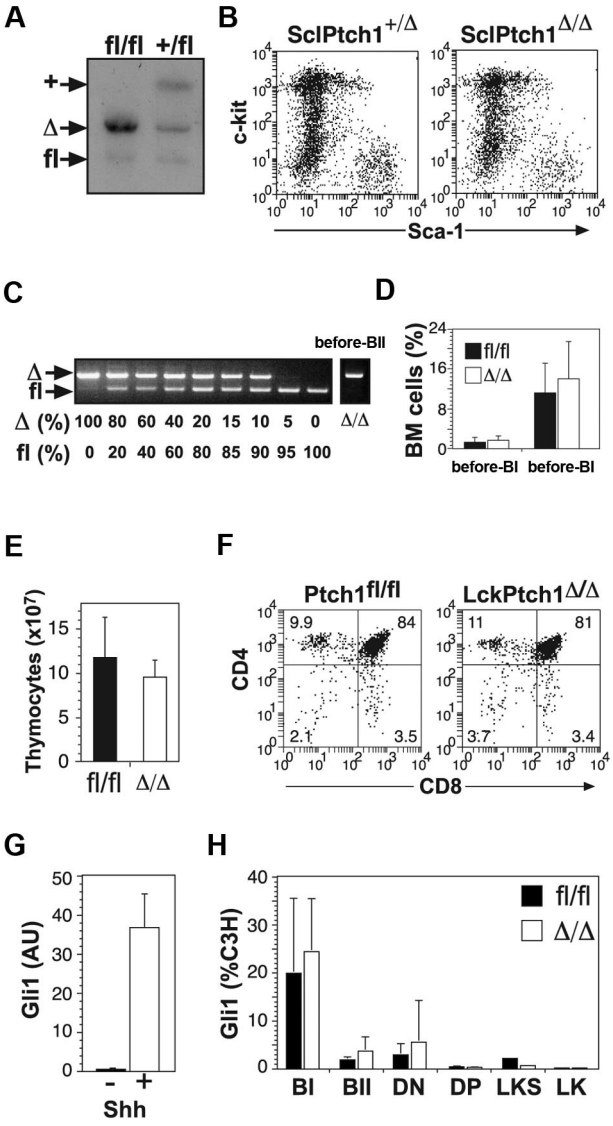

Figure 5. Hematopoietic-specific deletion of *Ptch1*. (A) *Ptch1* Southern blot of BM cells from *SclPtch1*$^{fl/fl}$ and *SclPtch1*$^{+/fl}$ mice 8 weeks after tamoxifen. Unlike all other blots, the probe used for this blot distinguishes *Ptch1* wild-type (+) and *Ptch1*^{fl} alleles. (B) Representative dot-plots of lineage-negative BM cells from *SclPtch1*-heterozygous (+/Δ) and *SclPtch1*-null (Δ/Δ) mice 8 weeks after tamoxifen. (C) PCR for efficiency of *Ptch1*^{fl} deletion in pre-BII cells FACS-isolated from a *CD19Ptch1*$^{\Delta/\Delta}$ mouse. Deletion efficiency is at least 80%, as determined by the dose titration curve shown on the left. (D) Pre-B cell subsets in BM from *Ptch1*$^{fl/fl}$ (fl/fl) and *CD19Ptch1*-null (Δ/Δ) mice. Mean plus SD calculated from 4 mice of each genotype. (E) Thymocyte cellularity of *Ptch1*$^{fl/fl}$ (fl/fl) and *LckPtch1*-null (Δ/Δ) mice. Mean plus SD calculated from 4 mice of each genotype. (F) Representative dot-plots of T-cell subsets. The mean percentage shown for each subset was calculated from 4 mice of each genotype. (G) Quantitative RT-PCR for Gli1 mRNA expression in the mesenchymal cell line C3H treated with or without conditioned media containing Shh. Mean plus SD for 3 independent experiments is shown. (H) Quantitative RT-PCR for Gli1 mRNA expression in FACS-isolated BM fractions (pre-BI, pre-BII, LKS, and LK) and thymocyte fractions (DN and DP) from control (*Ptch*$^{fl/fl}$) and *MxPtch1*-null (Δ/Δ) mice. Results for B- and T-cell subsets are mean plus SD of 2 independent sorts, and LKS and LK results are from a single sort from a pool of 5 mice of each genotype.

As the skin disease progressed, *MxPtch1*$^{\Delta/\Delta}$ mice became unwell and were killed by 8 to 10 weeks after poly(I:C). To explore the relationship between the hematopoietic abnormalities and skin disease, we examined hematopoiesis in mice where *Ptch1* was deleted using the keratin-specific Cre transgenic mouse strain *K14Cre*. This mouse strain expresses Cre recombinase in the basal cells of the epidermis and other stratified epithelia including the thymic epithelium.[20,30] As expected, *K14Ptch1*$^{\Delta/\Delta}$ mice developed

widespread basal cell carcinomas by 3 to 4 weeks of age, which was more extensive than that seen in *MxPtch1*$^{\Delta/\Delta}$ mice (Figure 7C). Remarkably, *K14Ptch1*$^{\Delta/\Delta}$ mice developed lymphoid defects similar to but more severe than those seen in *MxPtch1*$^{\Delta/\Delta}$ mice: *K14Ptch1*$^{\Delta/\Delta}$ mice had a 16-fold loss of BM pre-BII cells (Figure 7D) and a 7-fold loss of thymocytes (Figure 7E). In contrast, *K14Ptch1*$^{\Delta/\Delta}$ mice did not develop increased numbers of LKS (Figure 7F), splenomegaly, or neutrophilia (data not shown). Thus, activation of the Hh signaling pathway in epithelial cells is the likely mechanism of the lymphoid but not myeloid cell defects observed in *MxPtch1*$^{\Delta/\Delta}$ mice.

Although loss of osteoblasts may explain the B-cell defect seen in *MxPtch1*$^{\Delta/\Delta}$ mice, this was not the case in *K14Ptch1*$^{\Delta/\Delta}$ mice, where osteoblasts numbers were normal (Figure 7G). The T-cell defect observed in *K14Ptch1*$^{\Delta/\Delta}$ mice was also unlikely to be explained by an abnormality of the thymic cell niche because, unlike epithelial cells of the skin, thymic epithelial cells of *K14Ptch1*$^{\Delta/\Delta}$ mice were not increased (supplemental Figure 5). One possible mechanism for the lymphoid defects is elevated levels of epithelial-derived TSLP, a cytokine implicated in regulating B- and T-cell numbers. *TSLP* transgenic mice have very similar lymphoid defects to that seen in *MxPtch1*$^{\Delta/\Delta}$ and *K14Ptch1*$^{\Delta/\Delta}$ mice.[31] Consistent with this hypothesis, TSLP mRNA expression was increased 6-fold in the skin, but not thymus, of *MxPtch1*$^{\Delta/\Delta}$ mice (Figure 7H). Increased epithelial expression of TSLP led a 10- to 30-fold increase in circulating TSLP. Thus, activation of the Hh pathway in epithelial cells leads to markedly increased levels of circulating TSLP.

Discussion

We have used inducible and tissue-specific deletion of *Ptch1* to determine the cell-intrinsic and cell-extrinsic hematopoietic effects of activating the Hh pathway. Surprisingly, we found that deletion of *Ptch1* in hematopoietic cells, including HSCs, did not lead to activation of the Hh signaling pathway and consequently had no phenotypic effect. In contrast, deletion of *Ptch1* in nonhematopoietic cells produced 2 dramatic hematopoietic phenotypes: increased numbers of cycling LKS with increased circulating myeloid progenitors and apoptosis of B- and T-cell precursors. Deletion of *Ptch1* with an epithelial-specific Cre

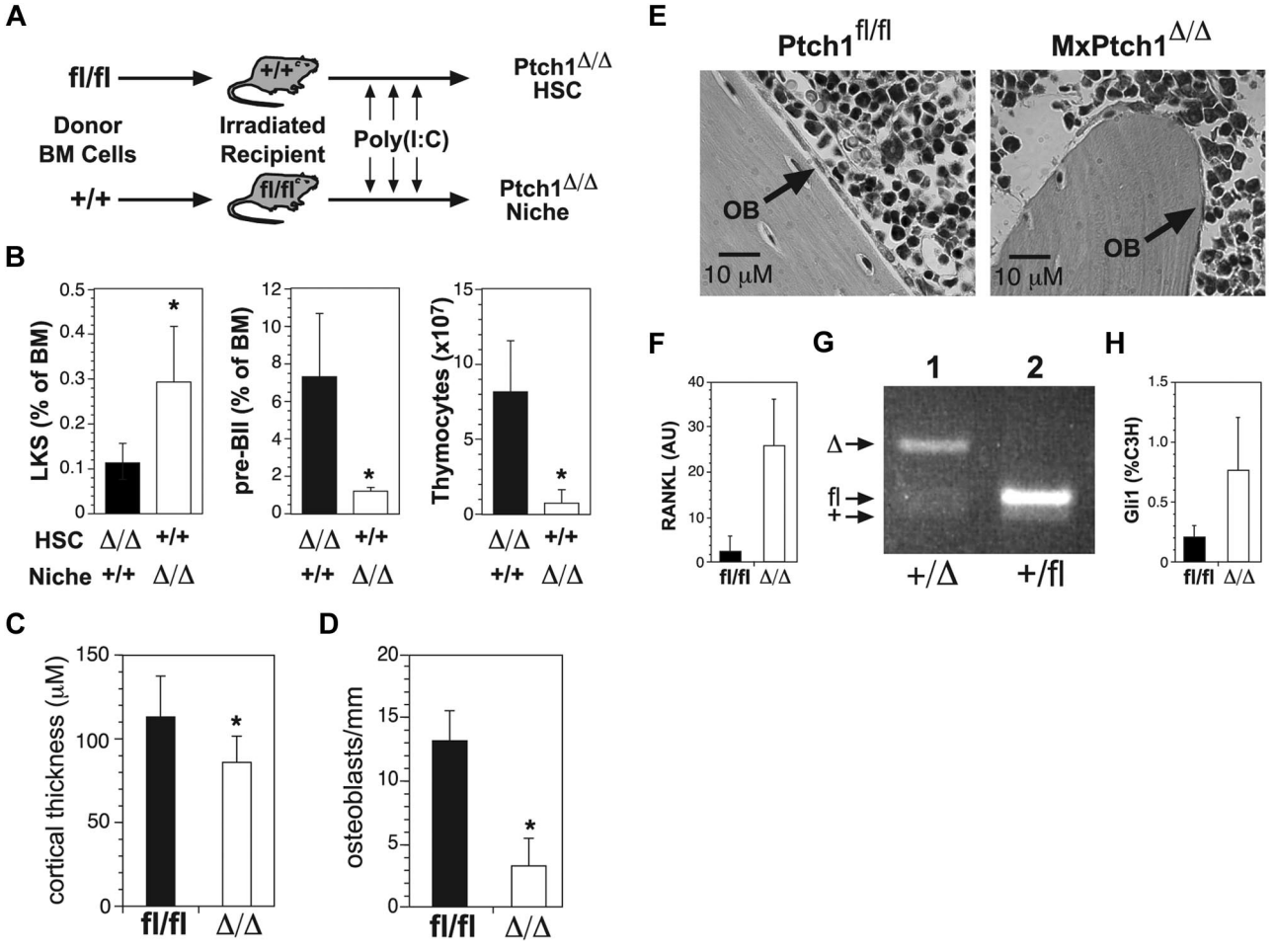

Figure 6. Hematopoietic abnormalities in *MxPtch1*$^{\Delta/\Delta}$ mice are cell-extrinsic. (A) Schematic of transplantation experiment. Donor BM cells from *MxPtch1*$^{fl/fl}$ or wild-type mice (+/+) were transplanted into lethally irradiated recipients. At 4 to 8 weeks after reconstitution, recipients were injected with poly(I:C) to generate either *Ptch1*-null hematopoietic cells or a *Ptch1*-null nonhematopoietic cells including the cell niche. (B) Numbers of LKS and B220^{lo}CD25^{+} pre-BII BM cells and thymocytes were measured 4 to 6 weeks after poly(I:C). Mean plus SD calculated from 4 recipients of each genotype. *$P < .05$ by 2-tailed Mann-Whitney test. (C) Mean cortical thickness plus SD through the mid-shaft of femurs from 3 mice of each genotype. *$P < .05$ by unpaired 2-tailed *t* test. (D) Numbers of osteoblasts along femoral shaft of *MxPtch1* mice. Mean plus SD from 3 mice of each genotype. *$P < .05$ by unpaired 2-tailed *t* test. (E) Histologic features of periosteum from trabecular bone of femurs from *MxPtch1* mice. OB indicates osteoblast. (F) Quantitative RT-PCR for RANKL mRNA expression in BM from MxPtch1 mice. Mean plus SD from 2 mice of each genotype. (G) PCR for *Ptch1*^{fl} deletion in sorted osteoblasts from *MxPtch1*$^{+/\Delta}$ mice (lane 1). As a control for nondeleted *Ptch1*^{fl} allele, BM cells from a *Ptch1*$^{+/fl}$ mouse is shown (lane 2). (H) Quantitative RT-PCR for Gli1 mRNA expression in whole bone samples from control (*Ptch*$^{fl/fl}$) and *MxPtch1*-null (Δ/Δ) mice. Results are mean plus SD of 3 mice of each genotype.

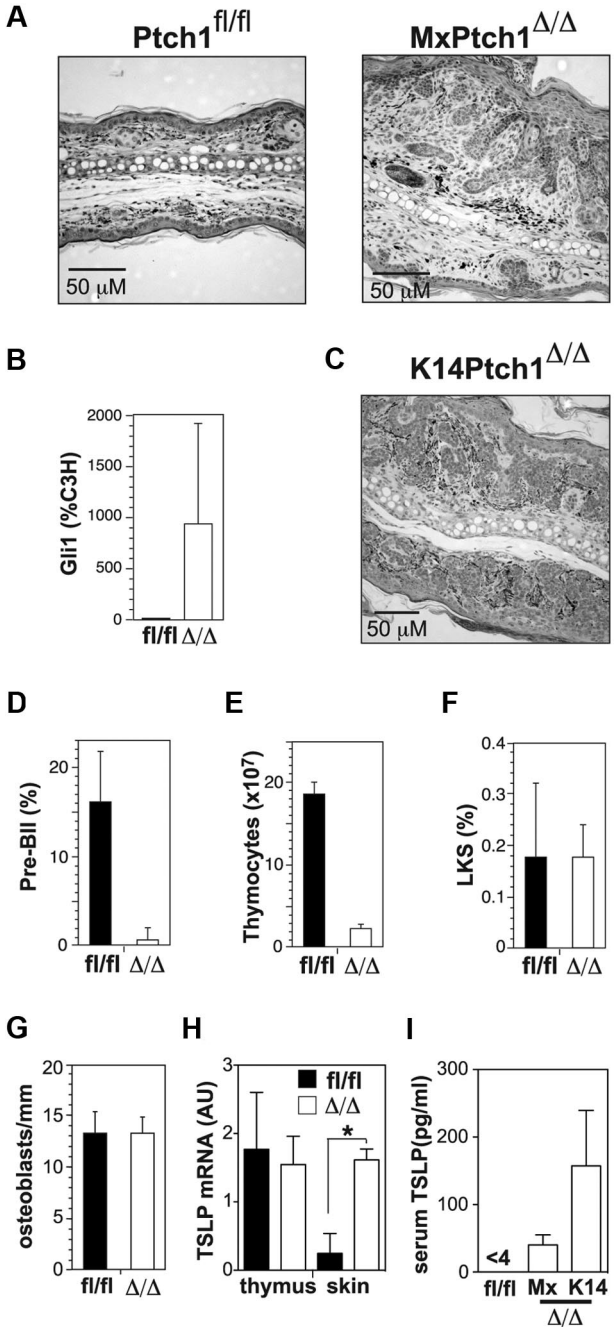

Figure 7. Deletion of *Ptch1* in epithelial cells causes the B- and T-cell defects. (A) Characteristic histologic appearance in skin of *MxPtch1*$^{\Delta/\Delta}$ mice. (B) Quantitative RT-PCR for Gli1 mRNA expression in skin from *MxPtch1*$^{\Delta/\Delta}$ mice. Mean plus SD from 3 mice of each genotype. (C) Characteristic histologic changes in skin of *K14Ptch1*$^{\Delta/\Delta}$ mice. (D) Numbers of pre-BII cells and (E) thymocytes in *K14Ptch1* mice. Analyses were performed at 4 to 6 weeks of age. Mean plus SD from 5 mice of each genotype. (F) Numbers of LKS cells in BM from *K14Ptch1* mice. Mean plus SD from 7 mice of each genotype. (G) Numbers of osteoblasts along femoral shaft of *K14Ptch1* mice. Mean plus SD from 3 mice of each genotype. (H) Quantitative RT-PCR for TSLP mRNA expression in thymus and skin of control (*Ptch*$^{fl/fl}$) and *MxPtch1-null* (Δ/Δ) mice. Results were normalized for HPRT and expressed as the mean plus SD (arbitrary units [AU]) from 3 mice of each genotype. (I) Serum TSLP levels in *MxPtch1*$^{\Delta/\Delta}$ mice (n = 4) and *K14Ptch1*$^{\Delta/\Delta}$ mice (n = 4). Serum TSLP levels in control *Ptch1*$^{fl/fl}$ mice (n = 8) were below the detectable limit of the immunoassay (4 pg/mL).

demonstrated that these 2 hematopoietic phenotypes are mediated by distinct cell-extrinsic mechanisms. Activation of the Hh signaling pathway in the BM cell niche led to loss of osteoblasts and increased LKS numbers, whereas activation of Hh signaling in epithelial cells led to increased circulating TSLP and death of lymphoid precursors.

Using a tamoxifen-inducible deletion of *Ptch1* in adult mice, Uhmann et al reported rapid loss of common lymphoid progenitors (CLPs), but they suggested that this defect was cell-extrinsic because *Ptch1*-null CLPs could grow in immunodeficient *Rag2*$^{-/-}$ $\gamma^{-/-}$ mice.[14] Our results provide significant insight into the mechanism of the lymphoid defects reported by Uhmann et al. First, we show that the loss of B and T cells is due to apoptosis of early lymphoid progenitors rather than defects in proliferation or differentiation. The normal numbers of pro-B cells (B220^{lo}CD19^{-}) in the BM of *MxPtch1*$^{\Delta/\Delta}$ mice suggest that Ptch1 is required for survival of pre-B cells rather than CLPs. Second, demonstration that wild-type HSCs have severe lymphoid abnormalities whentransplanted into *MxPtch1*$^{\Delta/\Delta}$ mice definitively proves the cell-extrinsic nature of these defects. Finally, identical lymphoid defects in *K14Ptch1*$^{\Delta/\Delta}$ mice strongly suggest that the cell-extrinsic mechanism is due to deletion of *Ptch1* in epithelial cells.

The phenotype of the *K14Ptch1*$^{\Delta/\Delta}$ mice suggests that the B- and T-cell defects are not due to defects of the cell niches regulating B- and T-cell progenitors. With respect to the B-cell defect, *K14Ptch1*$^{\Delta/\Delta}$ mice had normal numbers of osteoblasts. Furthermore, there is no evidence that the *K14Cre* transgene is expressed in the BM cell niche. With respect to the T-cell defects, we observed no expansion of thymic epithelial cells (supplemental Figure 5) despite the ability of the *K14Cre* to delete "floxed" genes in thymic epithelium.[20] One possible explanation for the lymphoid defects is an elevated level of epithelial-derived TSLP, which was observed in both *MxPtch1*$^{\Delta/\Delta}$ and *K14Ptch1*$^{\Delta/\Delta}$ mice (Figure 7H,I). *TSLP* transgenic mice have very similar lymphoid defects to that seen in *MxPtch1*$^{\Delta/\Delta}$ and *K14Ptch1*$^{\Delta/\Delta}$ mice.[31] However, it remains to be determined whether Hh signaling is a direct regulator of TSLP in epithelial cells and, if so, whether it is the direct cause of the lymphoid defects. Despite markedly elevated levels of circulating TSLP, we cannot exclude the possibility that apoptosis of pre-B cells and thymocytes are due to high levels of lymphotoxins observed in acute illness such as cortisol, TNF-α, and IFN-γ.[32]

Similar to the lymphoid defects, we show that expansion of LKS and mobilization of myeloid progenitors is caused by deletion of *Ptch1* in nonhematopoietic cells. Despite these changes, highly quantitative, competitive transplantation assays in congenic mice did not reveal any expansion or loss of HSC activity. Deletion of a single *Ptch1* allele in the adult had no demonstrable effects. This result contrasts with germline *Ptch1*-heterozygous mice, where elevated Gli1 mRNA in *Ptch1*-heterozygous LKS associated with HSC exhaustion were reported.[13] Possible explanations for these differences include the timing of *Ptch1* deletion (embryonic vs adult), the cell types affected (all cells compared with MxCre targeted cells) and the targeting strategy (start codon compared with first transmembrane domain). A similar discrepancy between germline and inducible deletion of *Ptch1* was reported for bone homeostasis.[33,34]

Our results do not definitively identify the target cell mediating the increased LKS and circulating myeloid progenitors in *MxPtch1*$^{\Delta/\Delta}$ mice. However, the loss of osteoblasts in *MxPtch1*$^{\Delta/\Delta}$ mice, but not *K14Ptch1*$^{\Delta/\Delta}$ mice, that have no LKS abnormality, makes osteoblasts a good candidate. It is hypothesized that more quiescent HSCs reside in the endosteal niche while more active cycling HSCs "primed" for mobilization reside in the vascular niche.[35] The increased cell cycling and mobilization of LKS in *MxPtch1*$^{\Delta/\Delta}$ mice would be consistent

with this hypothesis. We also found increased expression of RANKL, which may contribute to the loss of bone and increased progenitor cell mobilization in these mice.[27] The relative importance of the bone and vascular cell niches remains controversial although the normal HSC activity in *MxPtch1*$^{\Delta/\Delta}$ BM, despite the marked loss of osteoblasts, supports the recent studies of biglycan-deficient mice, which have reduced osteoblasts and trabecular bone yet normal HSC function.[36]

Loss of osteoblasts in *MxPtch1*$^{\Delta/\Delta}$ mice may be a direct effect of activation of the Hh signaling pathway because *MxCre* can excise the *Ptch1*^{fl} allele in osteoblasts (Figure 6G), and activation of Hh signaling in mesenchymal cells inhibits osteoblast differentiation.[37] Mak et al have also reported loss of postnatal bone after deletion of *Ptch1* in mature osteoblasts.[33] Our data suggest that targeting Hh signaling in bone might be a method of regulating HSC cell cycle without impairing long-term stem cell activity. This may be useful for enhancing hematopoietic recovery after chemotherapy or for sensitizing quiescent leukemic stem cells that reside in the endosteal cell niche.[38]

The observation that deleting *Ptch1* in hematopoietic cells did not lead to activation of the Hh signaling pathway has important implications for therapies that target Ptch1. Given that Hh proteins act by inhibiting Ptch1,[39] our results raise the possibility that the reported hematopoietic effects of Hh proteins are indirect through their effects on the microenvironment. For example, the enhanced ability of Ihh-expressing stroma to support HSCs may be indirect through changes to the stromal cells.[11] A similar effect of Hh proteins on the stromal microenvironment was shown to be important for maintaining the growth of epithelial tumors.[40] Alternatively, Ptch1 redundancy in hematopoiesis may be due to expression of Ptch2, which was expressed at normal levels in *MxPtch1*$^{\Delta/\Delta}$ myeloid and lymphoid progenitors (supplemental Figure 6), and can bind Hh proteins with similar affinity to Ptch1.[41] Hh agonists have been proposed for expansion of HSCs and improving BM regeneration after transplantation or chemotherapy. Although the HSC effects seen in *MxPtch1*$^{\Delta/\Delta}$ support this notion in part, our results highlight the importance of distinguishing direct from indirect effects of activating the Hh signaling pathway in hematopoiesis.

Acknowledgments

We thank Lan Ta, Rebecca Bowyer, and Jenny Davis for animal husbandry; Dean Hewish for cell sorting; and Natalie Sims for advice with analyses of bone, including histomorphometry.

This study was supported in part by research funding from National Health & Medical Research Council (NHMRC) to D.J.C. (Project Grant No. 435107; RD Wright Fellows 382904) and S.M.J. (Principal Research Fellow).

Authorship

Contribution: S.L.S. designed research, performed research, analyzed data, and wrote the manuscript; M.P.M. designed research, performed research, and analyzed data; S.M.J. performed research and wrote the manuscript); N-Y.N.N. performed research and analyzed data; S.V. performed research; D.J.C. performed research and wrote the manuscript; and R.V. and B.J.W. contributed new reagents.

Conflict-of-interest disclosure: The authors declare no competing financial interests.

Correspondence: David J. Curtis, Rotary Bone Marrow Research Laboratories, Royal Melbourne Hospital PO, Grattan St, Melbourne VIC 3050, Australia; e-mail: dcurtis@wehi.edu.au.

References

1. Wang Y, McMahon AP, Allen BL. Shifting paradigms in Hedgehog signaling. *Curr Opin Cell Biol.* 2007;19:159-165.
2. Gering M, Patient R. Hedgehog signaling is required for adult blood stem cell formation in zebrafish embryos. *Dev Cell.* 2005;8:389-400.
3. Mandal L, Martinez-Agosto JA, Evans CJ, Hartenstein V, Banerjee U. A Hedgehog- and Antennapedia-dependent niche maintains Drosophila haematopoietic precursors. *Nature.* 2007; 446:320-324.
4. Dierks C, Beigi R, Guo GR, et al. Expansion of Bcr-Abl-positive leukemic stem cells is dependent on Hedgehog pathway activation. *Cancer Cell.* 2008;14:238-249.
5. El Andaloussi A, Graves S, Meng F, Mandal M, Mashayekhi M, Aifantis I. Hedgehog signaling controls thymocyte progenitor homeostasis and differentiation in the thymus. *Nat Immunol.* 2006; 7:418-426.
6. Outram SV, Varas A, Pepicelli CV, Crompton T. Hedgehog signaling regulates differentiation from double-negative to double-positive thymocyte. *Immunity.* 2000;13:187-197.
7. Adolphe C, Narang M, Ellis T, Wicking C, Kaur P, Wainwright B. An in vivo comparative study of sonic, desert and Indian hedgehog reveals that hedgehog pathway activity regulates epidermal stem cell homeostasis. *Development.* 2004;131: 5009-5019.
8. Yang ZJ, Ellis T, Markant SL, et al. Medulloblastoma can be initiated by deletion of Patched in lineage-restricted progenitors or stem cells. *Cancer Cell.* 2008;14:135-145.
9. Ruiz i Altaba A, Mas C, Stecca B. The Gli code: an information nexus regulating cell fate, stemness and cancer. *Trends Cell Biol.* 2007;17:438-447.
10. Bhardwaj G, Murdoch B, Wu D, et al. Sonic hedgehog induces the proliferation of primitive human hematopoietic cells via BMP regulation. *Nat Immunol.* 2001;2:172-180.
11. Kobune M, Ito Y, Kawano Y, et al. Indian hedgehog gene transfer augments hematopoietic support of human stromal cells including NOD/SCID-beta2m$^{-/-}$ repopulating cells. *Blood.* 2004;104: 1002-1009.
12. Goodrich LV, Milenkovic L, Higgins KM, Scott MP. Altered neural cell fates and medulloblastoma in mouse patched mutants. *Science.* 1997;277: 1109-1113.
13. Trowbridge JJ, Scott MP, Bhatia M. Hedgehog modulates cell cycle regulators in stem cells to control hematopoietic regeneration. *Proc Natl Acad Sci U S A.* 2006;103:14134-14139.
14. Uhmann A, Dittmann K, Nitzki F, et al. The Hedgehog receptor Patched controls lymphoid lineage commitment. *Blood.* 2007;110:1814-1823.
15. Ellis T, Smyth I, Riley E, et al. Patched 1 conditional null allele in mice. *Genesis.* 2003;36:158-161.
16. Kuhn R, Schwenk F, Aguet M, Rajewsky K. Inducible gene targeting in mice. *Science.* 1995;269: 1427-1429.
17. Gothert JR, Gustin SE, Hall MA, et al. In vivo fate-tracing studies using the Scl stem cell enhancer: embryonic hematopoietic stem cells significantly contribute to adult hematopoiesis. *Blood.* 2005; 105:2724-2732.
18. Rickert RC, Roes J, Rajewsky K. B lymphocyte-specific, Cre-mediated mutagenesis in mice. *Nucleic Acids Res.* 1997;25:1317-1318.
19. Orban PC, Chui D, Marth JD. Tissue- and site-specific DNA recombination in transgenic mice. *Proc Natl Acad Sci U S A.* 1992;89:6861-6865.
20. Jonkers J, Meuwissen R, van der Gulden H, Peterse H, van der Valk M, Berns A. Synergistic tumor suppressor activity of BRCA2 and p53 in a conditional mouse model for breast cancer. *Nat Genet.* 2001;29:418-425.
21. Curtis DJ, Hall MA, Van Stekelenburg LJ, Robb L, Jane SM, Begley CG. SCL is required for normal function of short-term repopulating hematopoietic stem cells. *Blood.* 2004;103:3342-3348.
22. Metcalf D. *Haemopoietic Colony-stimulating Factors.* Amsterdam: Elsevier; 1984.
23. Kenney AM, Widlund HR, Rowitch DH. Hedgehog and PI-3 kinase signaling converge on Nmyc1 to promote cell cycle progression in cerebellar neuronal precursors. *Development.* 2004;131:217-228.
24. Schneider A, Zhang Y, Guan Y, Davis LS, Breyer MD. Differential, inducible gene targeting in renal epithelia, vascular endothelium, and viscera ofMx1Cre mice. *Am J Physiol Renal Physiol.* 2003;284:F411-417.
25. Calvi LM, Adams GB, Weibrecht KW, et al. Osteoblastic cells regulate the haematopoietic stem cell niche. *Nature.* 2003;425:841-846.

26. Zhu J, Garrett R, Jung Y, et al. Osteoblasts support B-lymphocyte commitment and differentiation from hematopoietic stem cells. *Blood.* 2007; 109:3706-3712.

27. Kollet O, Dar A, Shivtiel S, et al. Osteoclasts degrade endosteal components and promote mobilization of hematopoietic progenitor cells. *Nat Med.* 2006;12:657-664.

28. Walkley CR, Shea JM, Sims NA, Purton LE, Orkin SH. Rb regulates interactions between hematopoietic stem cells and their bone marrow microenvironment. *Cell.* 2007;129:1081-1095.

29. Zhang J, Niu C, Ye L, et al. Identification of the haematopoietic stem cell niche and control of the niche size. *Nature.* 2003;425:836-841.

30. Kuraguchi M, Wang XP, Bronson RT, et al. Adenomatous polyposis coli (APC) is required for normal development of skin and thymus. *PLoS Genet.* 2006;2:e146.

31. Osborn MJ, Ryan PL, Kirchhof N, Panoskaltsis-Mortari A, Mortari F, Tudor KS. Overexpression of murine TSLP impairs lymphopoiesis and myelopoiesis. *Blood.* 2004;103:843-851.

32. Wesche DE, Lomas-Neira JL, Perl M, Chung CS, Ayala A. Leukocyte apoptosis and its significance in sepsis and shock. *J Leukoc Biol.* 2005;78:325-337.

33. Mak KK, Bi Y, Wan C, et al. Hedgehog signaling in mature osteoblasts regulates bone formation and resorption by controlling PTHrP and RANKL expression. *Dev Cell.* 2008;14:674-688.

34. Ohba S, Kawaguchi H, Kugimiya F, et al. Patched1 haploinsufficiency increases adult bone mass and modulates Gli3 repressor activity. *Dev Cell.* 2008;14:689-699.

35. Kopp HG, Avecilla ST, Hooper AT, Rafii S. The bone marrow vascular niche: home of HSC differentiation and mobilization. *Physiology (Bethesda).* 2005;20:349-356.

36. Kiel MJ, Radice GL, Morrison SJ. Lack of evidence that hematopoietic stem cells depend on N-cadherin-mediated adhesion to osteoblasts for their maintenance. *Cell Stem Cell.* 2007;1:204-217.

37. Plaisant M, Fontaine C, Cousin W, Rochet N, Dani C, Peraldi P. Activation of Hedgehog signaling inhibits osteoblast differentiation of human mesenchymal stem cells. *Stem Cells.* 2009;3: 703-713.

38. Ishikawa F, Yoshida S, Saito Y, et al. Chemotherapy-resistant human AML stem cells home to and engraft within the bone-marrow endosteal region. *Nat Biotechnol.* 2007;25:1315-1321.

39. Ingham PW, McMahon AP. Hedgehog signaling in animal development: paradigms and principles. *Genes Dev.* 2001;15:3059-3087.

40. Yauch RL, Gould SE, Scales SJ, et al. A paracrine requirement for hedgehog signalling in cancer. *Nature.* 2008;455:406-410.

41. Carpenter D, Stone DM, Brush J, et al. Characterization of two patched receptors for the vertebrate hedgehog protein family. *Proc Natl Acad Sci U S A.* 1998;95:13630-13634.